Title

VHF-band Photoinjector: CBP Technical Note 366

Permalink

https://escholarship.org/uc/item/31f7t0vn

Authors

Staples, John
Sannibale, Fernando
Virostek, Steve

Publication Date

2006-10-26

CBP Tech. Note 366
October 26, 2006

VHF-band Photoinjector*

J. Staples, F. Sannibale, S. Virostek

Lawrence Berkeley National Laboratory
1 Cyclotron Rd., Berkeley CA 94720, USA

*This work was supported by the Director, Office of Science, Office of Basic Energy Sciences, of the U.S. Department of Energy under Contract No. DE-AC02-05CH11231.

CBP Tech Note 366

VHF-band Photoinjector

J. Staples, F. Sannibale, S. Virostek
Lawrence Berkeley National Laboratory

26 October 2006

Introduction

New generation accelerator-based x-ray light sources require high quality electron beams. Parameters such as transverse emittance (projected or “sliced”), energy spread and bunch length for beams in the nC charge range, need to be pushed beyond their present limits for the successful operation of light sources such as Energy Recovery Linacs (ERL) and Free Electron Lasers (FEL). At the same time, the demand for a high average brightness is also driving towards technologies capable of very high repetition rate operation. The overall performance is greatly determined at the accelerator injector and in particular, at the electron gun.

In this note, we present a new concept for a high repetition-rate photoinjector, capable of providing pulses up to at least 1 MHz or more. In order to achieve the experimental requirements, the requirements for the electron gun include:

- High brightness gun with bunch repetition rates up to ~1 MHz (dependent on cathode and laser system configuration)
- Compatible with easy installation and test of different cathodes
- Compatible with high repetition rate photocathode laser system capable of modification to test cathodes requiring different illuminating wavelength
- Variable bunch length at the photocathode from a few to several tens of picoseconds
- Compatibility with emittance compensation and manipulation techniques including the presence of magnetic fields at the photocathode
- $< 10^{-6}$ m normalized transverse beam emittance attainable downstream
- Charge per bunch of up to one nanocoulomb

New Concept: A VHF-band RF Gun

This is a novel scheme under development at LBNL that uses normal conducting RF structures operating in the frequency range between 50 to 100 MHz. The relatively low frequency allows for larger cavities with respect to the L and S band case leading to a dramatic reduction of the power density in the RF structure and allowing for CW operation of the gun. Lower frequencies mean also smaller accelerating gradients respect to the case of L and S band RF structures. Nevertheless, calculations show that this scheme has the potential to operate with very reasonable amount of RF power and achieve gradients and accelerating voltages larger than in the DC gun case. The long period of the RF is compatible with bunch length of tens of picoseconds, so from the point of view of the beam dynamics the VHF gun behaves as the static field case of DC guns and all the existing results from simulations and calculations for the DC gun case can be used for this VHF RF scheme. The relative large volume of the cavity allows for very good vacuum pumping speeds making the structure compatible with operation with photocathodes (GaAs for example) requiring extremely good vacuum conditions. The accelerating gap can be shaped in order to create focusing electric fields, and vacuum load lock techniques can be used for an "easy" replacement of the photocathodes. The overall size and complexity of the system compares favorably with DC gun based systems and in general, such VHF RF gun has the potential of achieving superior performance respect to DC guns using immediately available, mature, and conventional RF technology.

A VHF-band (30-300 MHz) normal conducting cavity is capable of supporting large voltages (0.5-1.0 MV) across gaps a few centimeters long resulting in 12-25 MV/m accelerating gradient with a significantly smaller dark current load than a DC gun. We are proposing to use a photoinjector based on a quarter-wave coaxial resonator operating in the 50-100 MHz region with a 4 cm accelerating gap. A summary of the parameters of the VHF-band photoinjector is listed in Table 1.

Figure 1 shows the configuration of the quarter-wave cavity. The structure is cylindrically symmetric around the beam axis with the photocathode at the end of the center conductor. The inner conductor provides sufficient room for a photocathode change mechanism, an electromagnetic solenoid to control the axial field at the photocathode surface and temperature control. The cavity is of all-metal construction designed to operate at a vacuum of less than 10^{-11} Torr. The photocathode is placed on the tip of the central conductor and the beam exits through a suitable extraction geometry to the right. For a 65 MHz resonant frequency, the axial length is 1 meter, the outer diameter is 1.4 meter, with a 0.3 meter diameter of the inner conductor. The end walls are dished to reduce deflection from atmospheric load and the entrance of the inner post is rounded to reduce tendency of multipactoring.

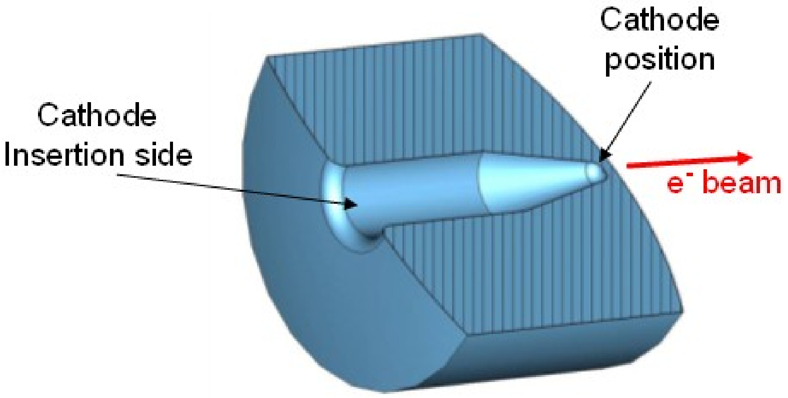

Figure 1. 3D cut-away view of the VHF normal conducting RF cavity for the photinjector

Table 1. Typical Cavity Parameters

Frequency	65	MHz
Gap Voltage	0.5-1.0	MV
Effective Gap Length	4	cm
Range of field in planar gap	12-25	MV/m
Cavity length	1	meter
Cavity diameter	1.4	meter
Inner conductor diameter	0.3	meter
RF power for 0.75 MV on gap	65	kW
Peak wall power density	7	W/cm^2
Vacuum	10^{-11}	Torr
Required pumping speed	25000	liter/sec
Construction	copper-plated aluminum	

CW RF power is introduced through a drive loop coupling with the large RF magnetic field at the base end of the center conductor. Typical operating Q_0 of such structures is in the range of $3.5\text{x}10^4$, requiring 29 kW CW for 500 kV across a 4 cm gap, or 65 kW for 750 kV across the gap at 65 MHz. Similar structures operating CW in storage rings sustain potentials of 1 MV across a 3 cm gap.

The cavity frequency is a harmonic N of the beam pulse rate, and is related to the linac frequency by a ratio of small integers. With suitable choice of frequency non-beam dark current is not synchronous with peak fields in the following linac. Beam pulse rates are not limited by the wall power density of the photoinjector in this concept, but rather by external elements such as the drive laser, photocathode heating, or beam loading in subsequent accelerator components. For example, if a 1 MHz, 1 nC beam pulse is accelerated to 750 keV, the beam loading of the structure itself is 750 watts, 1.2% the 65 kW needed to excite the cavity.

The geometry of the gap region will be optimized to minimize the extracted beam emittance. A planar 4-cm gap excited to 750 kV sustains a field of 18.7 MV/m. The final extraction geometry will be based on a modified Pierce configuration, designed to minimize the peak surface field and optimize the extracted beam characteristics.

At fields of 15-30 MV/m, dark current is not likely to be a problem. Dark current is significant at photocathode fields of the order of 60 MV/m, but field emission falls off somewhat faster than the field squared, reducing the dark current at 15-30 MV/m by more than an order of magnitude. In addition, dark current tends to have significantly different Twiss parameters, and much can be collimated out downstream of the injector.

It is expected that multipactoring will occur, as in all RF cavities, primarily in the rear region farthest away from the extraction end of the cavity. Methods of mitigation include breaking the symmetry in this region, which will happen by the inclusion of a drive loop and tuners, by modifying the surface to reduce secondary electron emission, and by including local magnetic fields to break up single-point multipactoring.

The low (VHF-band) operating frequency simplifies the manipulation of long (10's of picosecond) beam pulses. For example, 50 ps represents an RF phase advance of 1.2 degrees at 65 MHz, a typical operating frequency, imposing an energy chirp of less than 40 volts out of 750 kV if the pulse is centered on the RF peak (the transit time across a 4 cm, 750 kV gap is 205 picoseconds).

The quarter-wave structure is mechanically robust. The peak wall power density is 7.0 Watts/cm^2 at the base of the center conductor, much lower elsewhere. To maintain the frequency shift with a temperature rise of the central conductor to 20% of the 3-db cavity bandwidth, the temperature of the central conductor must be maintained to within 0.3 C if active tuners are not used (coarse tuners will be provided). The cavity is strictly locked to an small integer radio subharmonic of the linac RF system, so the RF amplifier need not be broad-banded, once the operating frequency is chosen.

A vacuum of 10^{-11} Torr in the vicinity of the photocathode is required. A conservative outgassing rate for treated and baked copper is 2.5×10^{-12} Torr-liter/sec cm^2. With an overall wall area of 7.5 m^2, a total pumping speed of 2×10^4 liter/sec is required. The large outer diameter of the structure provides good accessibility for ion- or cryo-pumps, and the all-metal structure is compatible with a high-temperature bake.

The further development of the VHF-band photoinjector concept will optimize the cavity geometry to further minimize the RF power requirement, simplify the tuning and frequency control, and to engineer space for the photoinjector components. RF amplifiers in this frequency range use off-the-shelf components and widely-available power tubes. Phase jitter of the RF is not a large concern, as the beam pulse depends on laser timing, much less on RF phase.

The RF power system to excite the VHF cavity can be based on broadcast transmitters for radio and television applications. These transmitter systems which uses tetrodes tubes and include power supplies, crowbar system, and control electronics are commercially available from multiple vendors.

Injector Cavity Thermal and Structural Analysis

The initial design concept for the coaxially configured injector cavity consists of an aluminum body with copper plating on the interior surfaces. The inner and outer conductors consist of 1 cm thick cylindrical shells that are 30 cm and 140 cm in diameter, respectively. The front and rear covers are made from thicker material and are dished to provide increased stiffness to minimize deflections due to the vacuum loads.

The front and rear covers will be bolted to the outer cavity cylinder by means of flanges containing RF and vacuum seals. The inner conductor and the tapered nose are to be welded to the rear cavity cover prior to plating and assembly. The tuner will be mounted on the rear cavity cover plate.

Approximately five 10" cryopumps, each with a pumping speed of 5000 l/s (H_2), will be mounted on the forward portion of cavity outer body and on the front cavity cover. The total interior cavity surface area is about 7.5 m^2.

A preliminary finite element analysis has been carried out using ANSYS to assess the thermal and structural performance of the cavity. Heat loads obtained from a Superfish RF analysis are applied to the cavity surfaces of the 2-dimensional, axisymmetric model. The 65 kW of total power dissipated in the cavity walls will be removed by means of cooling passages on the interior surface of the inner conductor and on the outside of the cavity. The 16 inner conductor channels (axially running), 16 outer cylinder channels (axially running) and one channel per end plate (circumferentially running) will carry a total flow of 51 gpm.

The thermal solution results in the temperature contour plot shown in Figure 2. The highest temperature reached in this case is 76ºC for 20ºC cooling water. Since the model is 2D axisymmetric, the effect of the discrete, axially running passages must be approximated by distributing an effective convection rate evenly on the appropriate surfaces.

The structural solution is obtained by changing the thermal elements to the corresponding structural equivalents. Loads applied to the model include the temperature profile and external atmospheric pressure. A contour plot showing the cavity deflections is shown in Figure 3. The maximum distortion of the cavity is less than 1 mm, and the change in the cavity gap is less than 0.5 mm. Neglecting the effects of stress concentrations, the stress was found to be approximately 27 MPa or about 10% of the material yield stress.

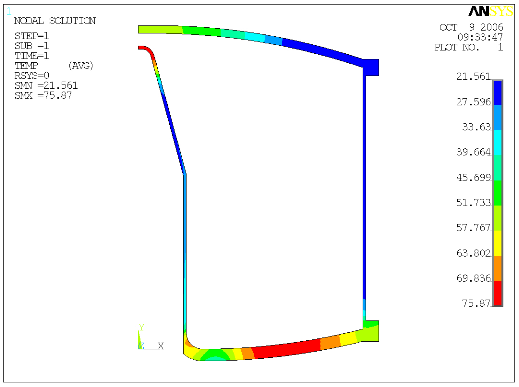

Figure 2: Cavity temperature contour (ºC).

Figure 3: Cavity displacement contour (m).